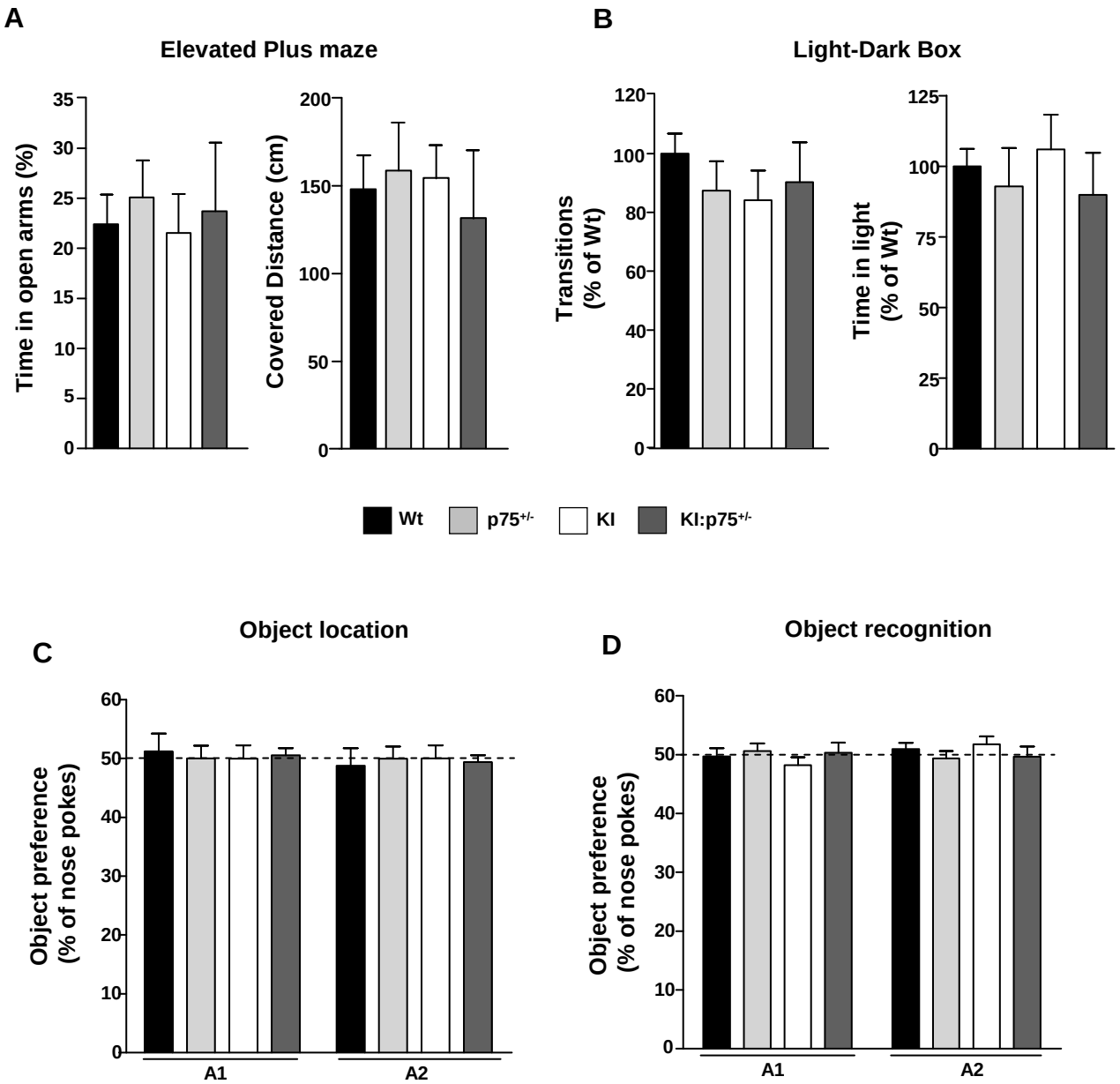

Supplemental Figure 1

Mutant KI mice do not exhibit anxiety-like behaviors. The plus maze and the light-dark box paradigms were used to evaluate anxiety-like behaviors in Wt, KI, p75+/- and KI;p75+/- at 6 months of age (n= 11-13). (**A**) In the elevated plus maze test, all genotypes spent similar percentage of time in the open arms and covered similar distance. (**B**) In the light-dark box, KI, p75+/- and KI;p75+/- mice made similar percentage of total transition to the light and spent similar time in the light compartment than Wt mice. Values are expressed as mean ± S.E.M. In the Novel object location task (**C**) and Novel object recognition task (**D**) all mice were first habituated to the open field arena and ambient conditions during three consecutive days and then subjected to a training session in the arena in the presence of two similar objects (A1 and A2). All genotypes similarly explored the object A1 and A2 indicating no object or place preferences in the animals.

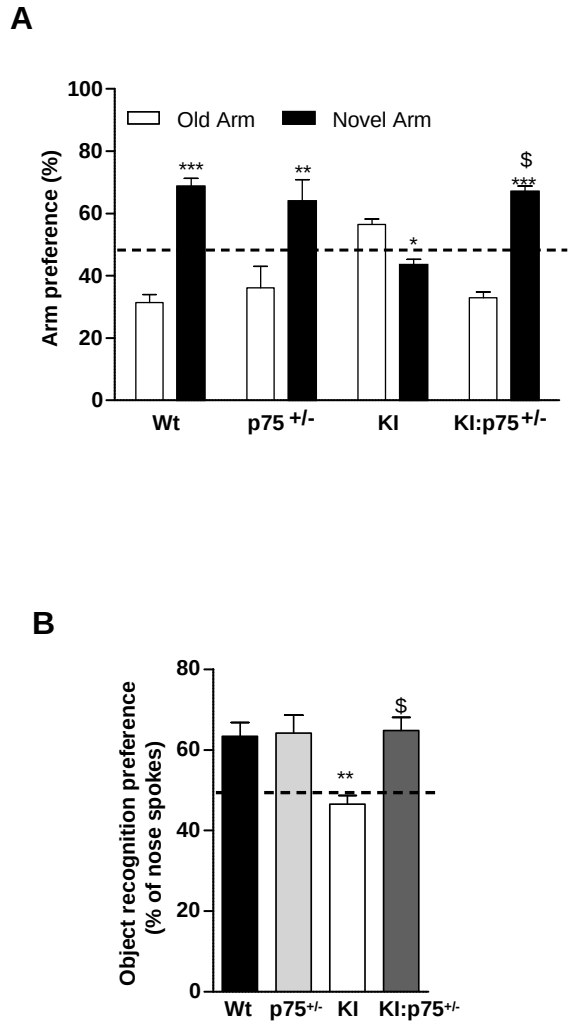

Supplemental Figure 2

Normalization of p75^{NTR} levels in mutant KI mice rescue hippocampal-dependent cognitive deficits at 8 months of age. (**A**) Percentage of time spent in arms (*old versus novel*) from Wt, p75+/-, KI and KI:p75+/- mice at 8 months of age (n = 8-12 per genotype). Mutant KI mice exhibit no preference for a previously unexposed (novel) arm of a T-maze. (**B**) Percentage of nose pokes to the new object from Wt, p75+/-, KI and KI:p75+/- mice at 8 months of age. One-way ANOVA with Bonferroni post hoc comparisons; * $p < 0.05$, ** $p < 0.01$ and *** $p < 0.001$ compared to Wt mice; $ $p < 0.05$, compared to KI mice. Data is presented as mean ± SEM.

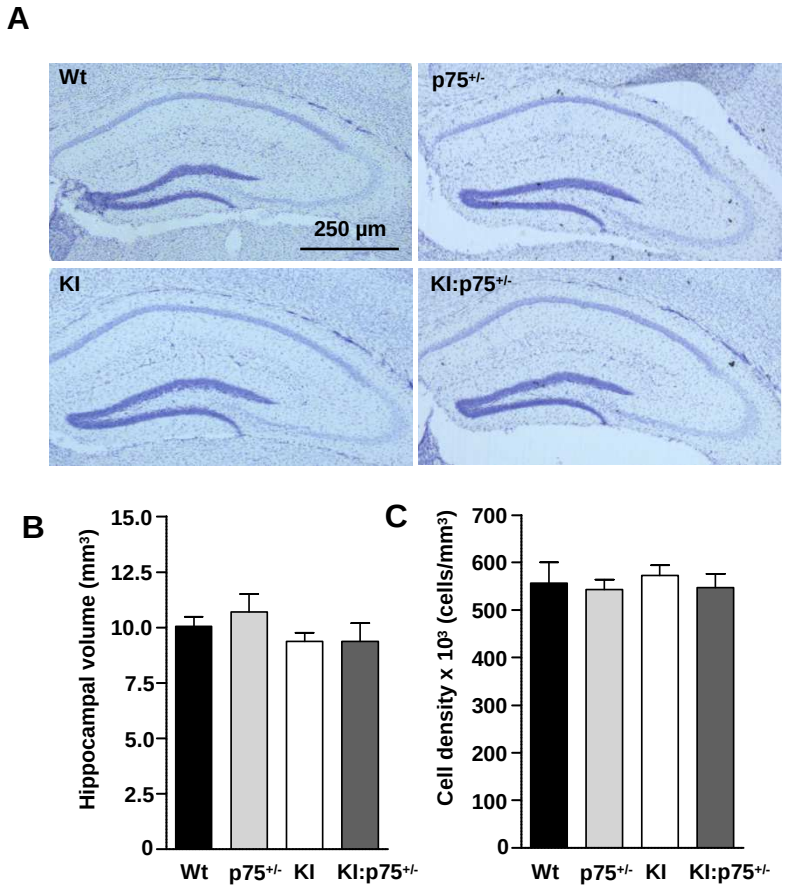

Supplemental Figure 3

Spared hippocampal gross anatomy in mutant KI mice. (**A**) Representative hippocampal coronal sections from Wt, p75+/-, KI and KI:p75+/- mice at 8 months of age stained with the Nissl method. (**B**) Total hippocampal volume and (**C**) cell density in the CA1 pyramidal cell layer from Wt, p75+/-, KI and KI:p75+/- mice at 8 months of age obtained by stereological counting and analysis. No significant differences between genotypes were found.

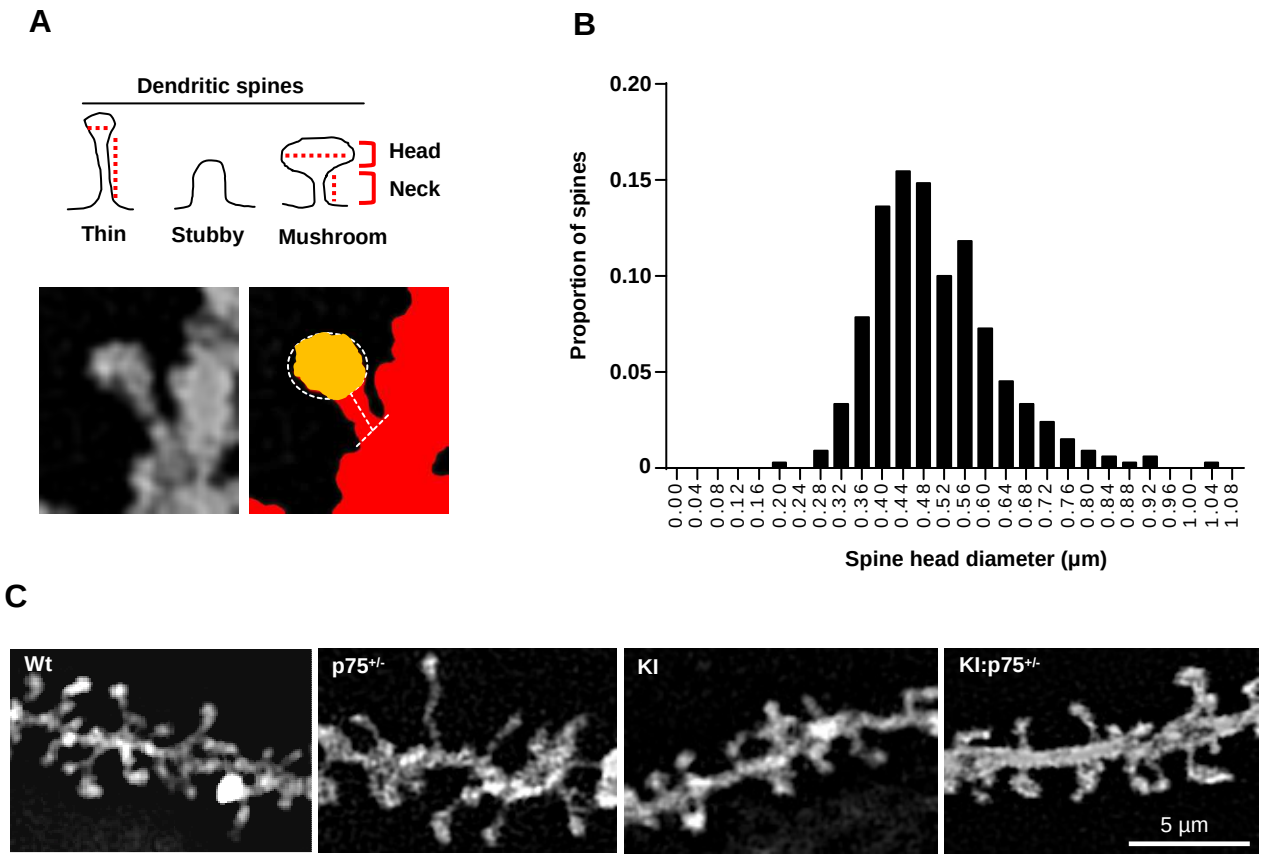

Supplemental Figure 4

Morphological analysis of dendritic spines. (A) Schematic drawing of spine morphologies in the categories as described in Harris and Stevens, 1989 (24). Enlarged image of a single spine is shown to represent the main parameters measured in the analysis: head diameter, area and neck length. **(B)** Frequency distribution of spine head diameter in Wt mice at 8 months of age. The Gaussian adjust results in a normal distribution with a mean value of 0,5009 ± 0,004 µm^2 (Gaussian fit r=0,90). **(C)** Representative confocal microscopy images showing DiI-stained basal dendrite segments of CA1 pyramidal neurons from Wt, KI, p75+/- and KI: p75+/-mice showing differences in the neck lengths.

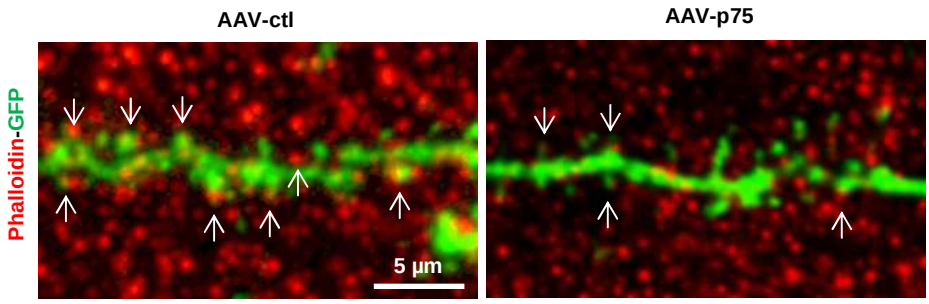

Supplemental Figure 5
Phalloidin colocalizes with GFP-positive dendritic spines in the CA1 hippocampal region. Double immunostaining for phalloidin (red) and GFP (green) in the stratum radiatum of the CA1 in AAV-ctl- and AAV-p75-infused Wt mice at 6 months of age. White arrows show double-labeled puncta for phalloidin and GFP. Note that AAV-p75-transduced neurons exhibit fewer spines.

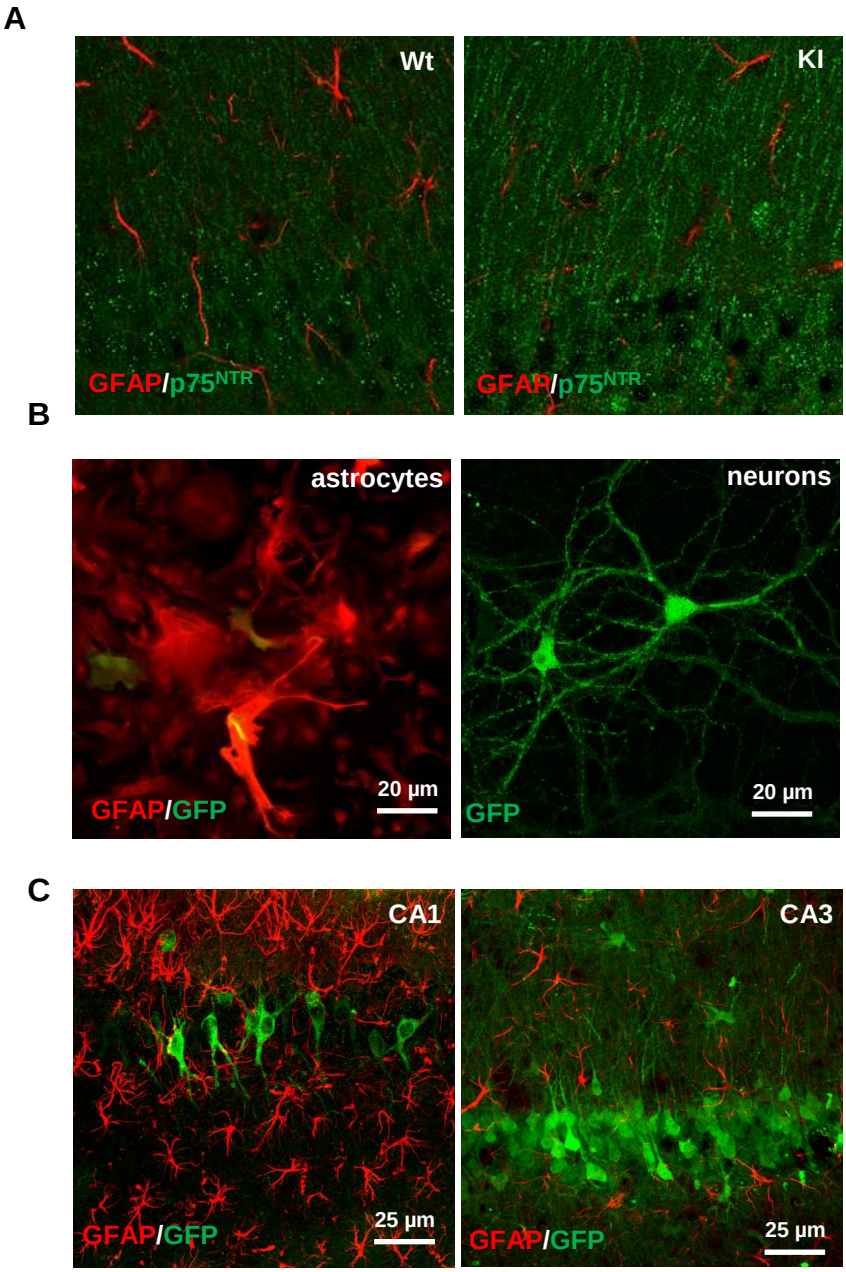

Supplemental Figure 6

p75^{NTR} expression is not found in astrocytes. (**A**) Representative confocal microscopy images showing lack of co-localization between p75^{NTR} and GFAP in the CA1 hippocampal region of Wt and KI mutant mice at 8 months of age. (**B**) Representative fluorescent microscopy images of AAV-p75GFP transduced astrocyte and hippocampal primary cultures showing GFP fluorescence and GFAP staining. Notice the lack of co-localization between GFP and GFAP in astrocyte primary cell cultures transduced with AAV-p75GFP. (**C**) Representative confocal microscopy images of CA1 and CA3 hippocampal regions showing GFP fluorescence and GFAP staining. Notice the absence of co-localization between GFP and GFAP in hippocampal slices injected with AAV-p75GFP.

Table S1. Protein levels of different synaptic-related proteins.

	Wt	KI	KI:p75$^{+/-}$
PSD95	100 ± 11,21	97,19 ± 11,34	164,1 ± 21,77*
PSD93	100 ± 8,11	84,24 ± 9,224	77,94 ± 10,52
Spinophilin	100 ± 7.967	117,7 ± 8,143	119,3 ± 18,76
SAP102	100 ± 14,64	82,99 ± 7,279	145,1 ± 16,20*
GluN1	100 ± 26.72	95.08 ± 7.064	118.4 ± 17.18
GluN2B	100 ± 14,22	123,6 ± 11,43	90,36± 15,41
GluA1	100 ± 7,095	102,9 ± 10,11	98,63 ± 9,68
GluA2/3	100 ± 13,88	121,88 ± 12,47	110,9 ± 11,47
Synaptophsyin	100 ± 5,35	95.40 ± 4.39	95.20 ± 2,22

Protein levels of synaptic-related proteins were analyzed by Western blot in protein extracts obtained from the hippocampus of Wt, KI and KI:p75$^{+/-}$ mice at 6 months of age (n = 6-7 per genotype). Data is presented as mean ± SEM. One-way ANOVA with Tukey *post hoc* comparisons were performed. * $p < 0.05$ compared to Wt mice.